

## Islanding and strain-induced shifts in the infrared absorption peaks of cubic boron nitride thin films

S. Fahy\*

*Department of Physics, University College, Cork, Ireland*

C. A. Taylor II and R. Clarke

*Department of Physics, University of Michigan, Ann Arbor, Michigan 48109-1120*

(Received 24 April 1997)

Experimental and theoretical investigations of the infrared-active, polarization-dependent phonon frequencies of cubic boron nitride films have been performed in light of recent claims that large frequency shifts during initial nucleation are the result of strain caused by highly nonequilibrium growth conditions. We show that the formation of small, separate grains of cubic boron nitride during the initial growth leads to a frequency shift in the infrared-active transverse-optic mode, polarized normal to the substrate, which is opposite in sign and twice the magnitude of the shift for modes polarized parallel to the substrate. In contrast, film strain causes a frequency shift in the mode polarized normal to the substrate, which is much smaller in magnitude than the frequency shift for modes polarized parallel to the substrate. Normal and off-normal incidence absorption measurements, performed at different stages of nucleation and growth, show that large frequency shifts in the transverse-optic-phonon modes during the initial stage of growth are not compatible with the expected effects of strain, but are in large part due to nucleation of small isolated cubic BN grains which coalesce to form a uniform layer. Numerical results from a simple model of island nucleation and growth are in good agreement with experimental results. [S0163-1829(97)06440-0]

### I. INTRODUCTION

Although the growth of cubic BN was first demonstrated<sup>1</sup> using a variety of catalysts at high temperature and pressure, recent efforts have concentrated on thin film deposition processes. A common feature of cubic BN deposition processes is the use of an energetic plasma to promote the growth of the cubic phase.<sup>2-7</sup> Boron nitride films grown under these highly nonequilibrium conditions undergo an unusual series of transitions leading to an amorphous-hexagonal-cubic layer structure.<sup>8</sup> Interestingly, the hexagonal layer is found to orient with the  $c$  axis parallel to the substrate surface. Using a thermodynamic free-energy analysis involving biaxial film stress, McKenzie<sup>9</sup> showed that the highly compressible  $c$  axis of hexagonal BN should orient parallel to the substrate surface to accommodate in-plane film strain, and also suggested that the buildup of unannealed defects generates sufficient internal film stress to reach the regime in the phase diagram where cubic BN is stable. Several researchers have since reported that cubic BN formation either scales<sup>10</sup> with or, is linked<sup>6,8,11</sup> to, compressive stress. Yet there seems to be little evidence to differentiate between cubic BN forming as a consequence of compressive stress or forming in conjunction with it. In a recent publication,<sup>12</sup> Friedmann *et al.* used Fourier transform infrared (FTIR) spectroscopy to study the initial nucleation of the cubic phase, and reported a large (positive) shift in the zone-center cubic TO-phonon frequency which decreased to an equilibrium value as growth continued. They propose that this frequency shift is consistent with high compressive stress during the initial nucleation of the cubic phase, and that it supports the transition mechanism proposed by McKenzie.

In this paper we examine the mechanism for phonon fre-

quency shifts during the nucleation and growth of cubic BN. We show that, while the zone-center TO frequency is sensitive to strain, it is also highly sensitive to geometrical factors during initial nucleation. We find that the available normal-incidence infrared spectroscopy data can be explained simply by a phenomenological theory which demonstrates the effect of island nucleation and coalescence on the frequencies of transverse-optic phonons. Moreover, we find that off-normal-incidence infrared-absorption measurements allow us to differentiate clearly between frequency shifts caused by strain and those due to geometrical factors arising during the initial formation of isolated crystallites. When off-normal-incidence data are taken into account, the very large shifts in the phonon frequencies which occur at the initial stages of growth are clearly not compatible with the expected effects of strain proposed by Friedman *et al.*,<sup>12</sup> but are in large part due to island formation and coalescence.

The effects of boundary conditions on the mode frequencies in small crystallites were considered by Fröhlich<sup>13</sup> as early as 1949. An extensive review of early theoretical and experimental results is given by Ruppin and Englman.<sup>14</sup> More recently, such effects have been of great interest in confined semiconductor structures (e.g., quantum-wells,<sup>15</sup> quantum dots,<sup>16</sup> and microcrystallites<sup>17</sup>). In general, it is found that the depolarizing electric field which gives rise, for example, to the LO-TO splitting for bulk modes in heteropolar materials, is strongly dependent in small samples on the geometry of the material and the mode excited.<sup>14</sup>

The simplest instance of such geometry or sample boundary effects in the present experiment is seen in the infrared absorbance spectrum measured at off-normal incidence for the case of thicker, uniform cubic boron nitride films. At off-normal incidence, infrared radiation couples to lattice

modes with polarization normal to the film surface. Because of the depolarizing field due to the induced surface charges, this mode appears at the bulk LO mode frequency,<sup>18</sup> although it is not a longitudinal mode. (It propagates along the film and so has a polarization perpendicular to its propagation wave vector.) This is the simplest example of the effects of surface geometry on the TO mode frequencies.

The remaining sections of this paper are organized as follows. In Sec. II we present the measurements of normal and off-normal-incidence infrared absorbance of BN thin films at various stages of film growth. Section III gives an analysis of the effects of grain geometry during cubic BN nucleation and growth on the infrared-active mode frequencies for polarizations normal and parallel to the substrate. In Sec. IV we analyze the effects of strain on the cubic BN infrared-active mode frequencies. We discuss the significance and implications of the combined experimental and theoretical results in Sec. V.

## II. EXPERIMENTAL RESULTS

Cubic boron nitride films were grown on Si(100) substrates by an rf magnetron sputter deposition process.<sup>5</sup> During growth, the substrates were biased negatively with respect to the ground, and were immersed in a nitrogen plasma produced by an electron cyclotron resonance (ECR) source. The growth temperature for this series of samples was 1100 °C and the nitrogen ion current, measured at the sample using a Faraday cup, was 0.9 mA/cm<sup>2</sup>. Optimum conditions for initiation of *c*-BN growth were found with a substrate bias of -80.0 V, and the film growth rate was measured to be  $\approx 4.5$  Å/min for the cubic material (7.2 Å/min for the hexagonal material). Infrared-absorption spectra were collected with 2-cm<sup>-1</sup> resolution using a nitrogen purged Nicolet Magna 550 Series II FTIR spectrometer. A bare silicon substrate, from the same wafer as the sample substrates, was used for background subtraction from the sample spectra.

Films grown under the conditions outlined above, with a thickness ranging from approximately 2000 to 4500 Å, were characterized structurally using both plan view and high-resolution transmission electron microscopy (TEM). The cross-section electron-diffraction patterns indicate an oriented hexagonal layer, with the *c* axis parallel to the substrate surface, and *c*-BN crystallites oriented in a [111] texture around the substrate normal. The high-resolution cross sections also reveal an amorphous-hexagonal-cubic layer structure similar to that reported in the literature.<sup>8</sup>

A series of much thinner films, with a total film thickness ranging from approximately 450 to 800 Å, was characterized using scanning force microscopy (SFM). The SFM images (see Fig. 1) reveal that the cubic BN layer initially nucleates on the hexagonal BN layer as highly aligned triangular crystallites. The triangular crystallites appear to nucleate at random locations on the surface, but remain highly aligned in the thinnest films. As growth continues, the triangular islands are seen to coalesce into a uniform layer with an average crystallite size of approximately 700 Å. The first continuous layer is very smooth, with a rms roughness on the order of 20 Å. Further growth continues with crystallites of similar size and shape nucleating on top of one another, but the orienta-

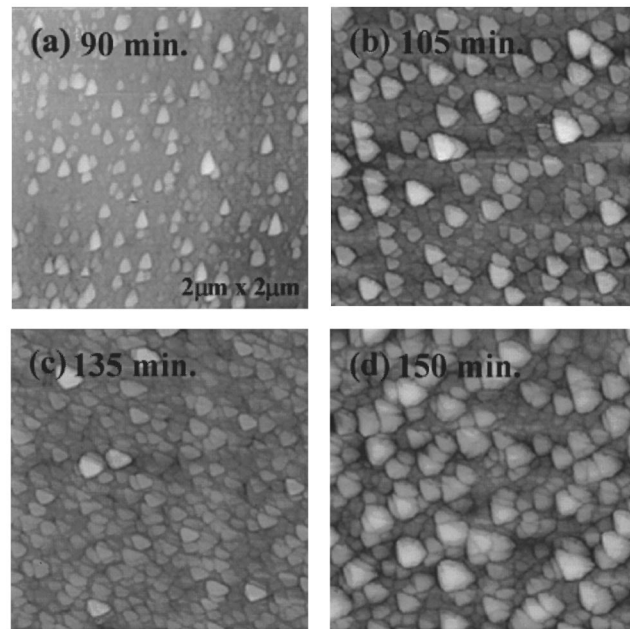


FIG. 1. Scanning force microscopy images of  $2 \times 2$ - $\mu\text{m}^2$  areas of the surface of boron nitride thin films at various stages of growth. The films are identified by total growth time, which includes the growth time for the amorphous and hexagonal BN layers.

tion becomes more random and roughness increases.

The triangular crystallites observed in the SFM images of very thin films are strongly suggestive of [111] crystal planes, which would indicate that the cubic BN initially nucleates with the [111] axis normal to the film surface, or more specifically, normal to the hexagonal BN [0002] (*c* axis). The orientation appears to become more random as growth continues, which is consistent with TEM diffraction results from thick films. While the orientational effects we observe are extremely interesting and require further investigation, the most important information to be taken from these images is that the cubic BN nucleates as isolated crystallites which coalesce to form a uniform film as growth continues.

Figure 2 shows infrared-absorption spectra collected at normal incidence for this same series of samples at different stages of growth. Spectra were measured at room temperature, after the growth of each sample was complete. The absorption peak which increases and shifts with growth time is the cubic BN zone-center TO-phonon mode with polarization parallel to the film surface. The frequency of this mode is typically cited as 1065 cm<sup>-1</sup> in bulk cubic BN crystals.<sup>19</sup> The absorption peaks near 770 and 1380 cm<sup>-1</sup> are BN TO-phonon absorptions<sup>20</sup> from the amorphous and oriented hexagonal layers in the film. Peak positions, determined from a computer-generated fit to the entire absorption spectrum, are listed in Table I (top half).

The frequency of the cubic TO mode is plotted in Fig. 3 as a function of cubic BN growth time. High-resolution TEM cross sections indicate that cubic BN growth begins when the hexagonal BN layer is approximately 300 Å thick, i.e., approximately 40 min after deposition begins. Included in this figure are data from thick samples grown to over 3000 Å. We observe that the cubic TO mode is shifted to higher frequency at the initial nucleation stage, and rapidly de-

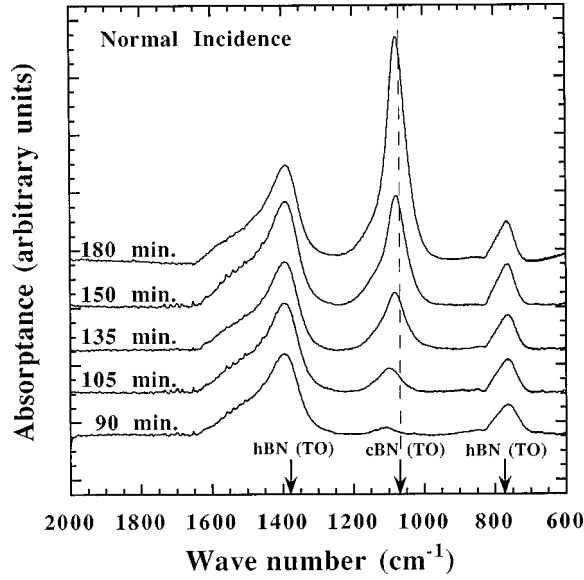


FIG. 2. Infrared-absorption spectra of boron nitride films measured at normal incidence. The films are identified by total growth time which includes the growth time for the amorphous and hexagonal BN layers.

creases to a minimum value, slightly above that of bulk cubic BN. This is similar to the findings of Friedmann *et al.*,<sup>12</sup> who attributed this shift to intrinsic film stress, suggesting that nucleation of the cubic phase occurs as a result of extremely high stress. In Sec. V, below, we will offer an alternative explanation for the initial large frequency shifts based on geometrical factors during the nucleation and coalescence of individual cubic BN grains on the substrate.

The absorption peaks observed at normal incidence are well reproduced in the infrared absorbance at off-normal incidence for films in the initial stages of cubic BN nucleation and growth. Shown in Fig. 4 are absorption spectra collected with the IR beam incident  $60^\circ$  from the sample normal. In this geometry two additional TO modes, at  $1618$  and  $1305$   $\text{cm}^{-1}$ , appear in the spectra. While these modes are strictly TO with mode polarizations perpendicular to the surface,<sup>18</sup> they appear near the LO frequencies of bulk

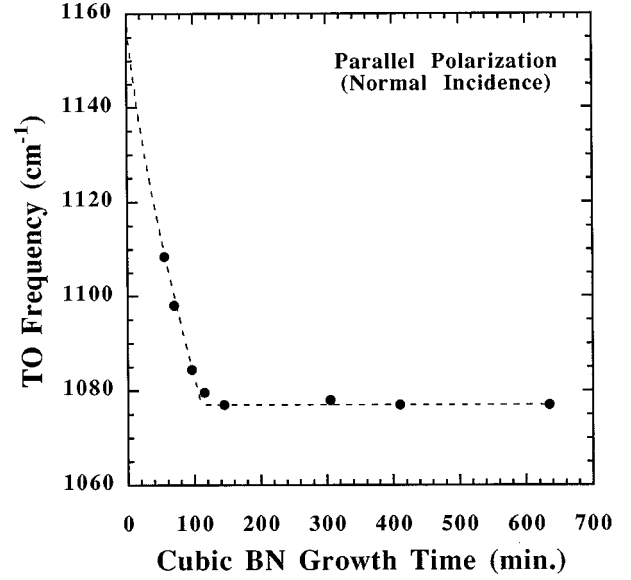


FIG. 3. Frequency of the cubic BN zone center TO mode as a function of cubic BN growth time. The points are the experimental absorption peak positions and the dashed line is a plot of  $\omega_{x,y}$  from Eq. (4a), using a coalescence time  $t_c = 110$  min and a (strain shifted) bulk TO frequency of  $1077$   $\text{cm}^{-1}$ .

hexagonal<sup>21</sup> ( $h$ -BNLO is equal to  $1610$   $\text{cm}^{-1}$ ) and cubic<sup>22,23</sup> BN ( $c$ -BNLO is equal to  $1305$   $\text{cm}^{-1}$ ), respectively. The peak positions of the LO peaks in the spectra are listed in Table I (bottom half).

### III. THEORY OF SHIFTS DUE TO ISLANDING

We now consider the effects of islanding (i.e., the formation of separate, individual cubic BN grains) on the infrared-absorption peaks during the initial stages of growth. In particular, using a simple model of the IR modes and the island geometry, we will show that the relation

$$\omega_z^2 - \omega_L^2 = -2(\omega_{x,y}^2 - \omega_T^2) \quad (1)$$

TABLE I. Peak positions from the infrared absorption spectra taken at normal (top half of the table) and off-normal incidence (bottom half). The peak shift ratio calculated for the off-normal incidence spectra assumes (see text) that the cubic TO peak position is affected by the residual strain (i.e.,  $\Delta\omega_T = \omega_T - 1077$   $\text{cm}^{-1}$ ).

Growth time (min.)	hex BN LO mode ( $\text{cm}^{-1}$ )	hex BN $E_{1u}$ mode ( $\text{cm}^{-1}$ )	cubic BN LO mode ( $\text{cm}^{-1}$ )	cubic BN TO mode ( $\text{cm}^{-1}$ )	hex BN $A_{2u}$ mode ( $\text{cm}^{-1}$ )	Shift ratio $\Delta(\omega_L^2)/\Delta(\omega_T^2)$
90		1376		1112	766	
105		1376		1094	766	
135		1376		1084	766	
150		1376		1078	767	
180		1376		1077	767	
90	1619	1376	1249	1113	767	2.1
105	1619	1376	1279	1093	766	2.0
135	1619	1376	1293	1084	766	2.1
150	1617	1376	1299	1078	767	7.3
180	1617	1376	1304	1077	767	n.a.

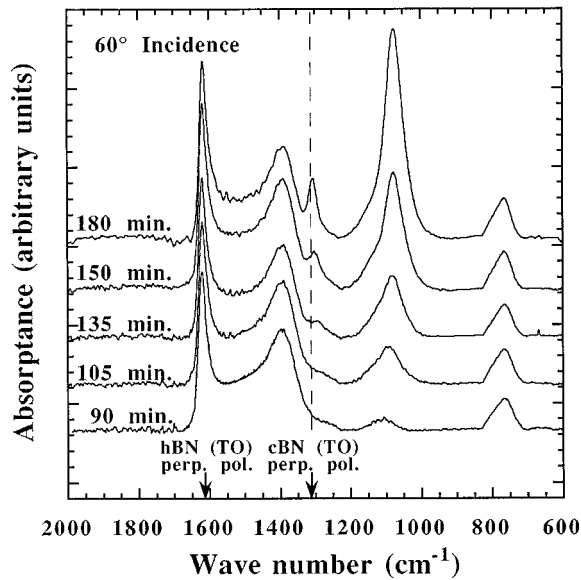


FIG. 4. Infrared-absorption spectra of boron nitride films measured at 60° off-normal incidence. The two additional peaks which appear in the spectra are TO modes with mode polarization perpendicular to the film surface.

approximately holds, where  $\omega_z$  is the mode frequency for polarization normal to the substrate, and  $\omega_{x,y}$  is the frequency for polarizations parallel to the substrate. For the purposes of this analysis, we assume initially that no shifts are caused by strain, by chemical impurities, or by non-stoichiometric composition of the cubic BN. Then, in Sec. IV, we will take the effects of strain into account explicitly.

We assume that we are dealing with a zone-center (infinite wavelength) phonon mode, and that the mode amplitude is approximately constant throughout each cubic BN grain. This is true if the grain shape can be approximated by an ellipsoid.<sup>13,14</sup> We also assume that the mode amplitude is the same for all grains on the substrate, neglecting electromagnetic retardation effects. This amounts to the approximation that the wavelength of the infrared light is substantially greater than the distance between grains of cubic BN on the substrate.

The macroscopic depolarization field  $\epsilon$  within each grain (which is proportional to the polarization density  $P$  within the grains) gives rise<sup>24</sup> to a shift in the mode frequency  $\omega$ . Then  $\omega^2 - \omega_T^2$  is proportional to the depolarization factor  $N = -\epsilon/P$ . The depolarization factor depends<sup>14,25</sup> on the shape of the individual grains, the electronic polarizability of the media (i.e., vacuum, hexagonal BN, and Si) near the grains, and the distribution of grains on the substrate. Moreover,  $N$  is different for modes with polarization normal to the substrate than it is for modes with polarization parallel to the substrate.

For a uniform layer,<sup>18</sup>  $N=0$  for modes polarized parallel to the substrate, and the phonon frequency equals the bulk TO frequency  $\omega_T$ . In the same geometry,  $N=4\pi$  for the mode polarized normal to the substrate, and the phonon frequency equals the bulk LO frequency  $\omega_L$ . Thus, in general, we have that

$$\omega^2 - \omega_T^2 = \frac{N}{4\pi} (\omega_L^2 - \omega_T^2). \quad (2)$$

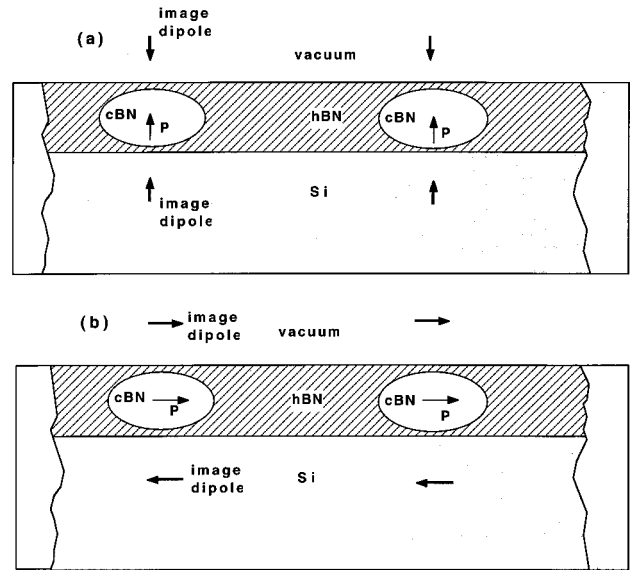


FIG. 5. A schematic section showing the initial growth of cubic BN (c-BN) grains within the hexagonal BN (h-BN) layer on a silicon substrate, indicating the cubic BN polarization  $P$  for IR modes polarized (a) normal to the substrate and (b) parallel to the substrate. The equivalent image dipoles (see text) for surface charges induced on the hexagonal BN-vacuum and hexagonal BN-silicon interfaces are indicated by the arrows below and above the grains.

As the individual islands coalesce to form an approximately uniform layer, the observed frequencies tend to the limits  $\omega_T$  and  $\omega_L$  for modes polarized parallel and perpendicular to the substrate, respectively. We expect this limit to be reached when the grain size is approximately equal to the distance between grains on the substrate.

Shown in Fig. 5 is a schematic section of the cubic BN grains on the silicon substrate during the initial state of growth. We may consider the depolarization field  $\epsilon$  within each grain, and hence the shift  $\omega^2 - \omega_T^2$  in Eq. (2), as arising from three sources: (1) the field due to the induced surface charge density on the cubic BN grain; (2) the field due to the surface charges induced on the hexagonal BN-silicon and hexagonal BN-vacuum interfaces; and (3) the electric dipole fields from the other cubic BN grains on the substrate.

In order to estimate contribution (1), we approximate the cubic BN grain by an ellipsoid of revolution of appropriate aspect ratio with its axis normal to the substrate. We assume that the cubic BN is surrounded by hexagonal BN (as indicated by the TEM cross sections), and neglect the small difference between the optical dielectric constant ( $\epsilon=4.5$ ) of hexagonal BN and that of cubic BN. We then use the standard result<sup>25</sup> that the depolarization factors  $N_x$ ,  $N_y$ , and  $N_z$  of any ellipsoid for polarization along the principal axes  $x$ ,  $y$ , and  $z$ , respectively, satisfy the relation  $N_x + N_y + N_z = 4\pi$ . Since  $N_x = N_y$ , then  $N_z = 4\pi - 2N_{x,y}$ , where  $N_z$  and  $N_{x,y}$  are the depolarization factors for the modes polarized normal and parallel, respectively, to the substrate.

To estimate contribution (2) of the induced charge on the hexagonal BN-silicon and hexagonal BN-vacuum interfaces, we use the method of images, as applied to planar interfaces between dielectric media.<sup>26</sup> We can then approximate the field due to the interface charges with those of image dipoles

above and below the interfaces, as shown in Fig. 5. The depolarization field at the cubic BN grain is that of dipoles oriented as in Fig. 5(a) for normal polarization, and as in Fig. 5(b) for parallel polarization. At a given distance from a dipole, the field is twice as large along the axis of the dipole as it is in the equatorial plane.<sup>27</sup> Thus the depolarization field from the interface charges for normal polarization of the phonon mode is approximately twice as large (and opposite in sign) as that for polarization parallel to the substrate. Adding contributions (1) and (2), we see that the depolarization factors again satisfy  $N_z = 4\pi - 2N_{x,y}$ , as for contribution (1) alone.

Finally, contribution (3) to the depolarization field due to the other cubic BN grains distributed on the substrate may be calculated as follows: The other cubic BN grains are randomly distributed on the surface, and their polarization is parallel to that of the grain for which we are calculating the depolarization field. Thus this contribution to the depolarization field is that of a set of parallel dipoles randomly distributed over the substrate, excluding the area occupied by the grain for which we are calculating the depolarization field. The average contribution to the depolarization field due to dipoles randomly distributed in an annulus of thickness  $dr$  at a distance  $r$  from the grain is equal to

$$d\varepsilon_{x,y} = \frac{1}{2} \frac{p_s}{r^3} 2\pi r dr \quad (3a)$$

for polarization parallel to the substrate, and

$$d\varepsilon_z = -\frac{p_s}{r^3} 2\pi r dr \quad (3b)$$

for polarization normal to the substrate, where  $p_s$  is the average dipole strength per unit area of the surface. Thus, with the inclusion of this contribution from the other grains to the depolarization field, we again find that the relation  $N_z = 4\pi - 2N_{x,y}$  between the depolarization factors remains valid.

Substituting this relation into Eq. (2), we obtain the result given in Eq. (1). Much of the argument which leads to this conclusion is not specific to cubic BN, and should be applicable to many wide-band-gap polar semiconductors or insulators growing on silicon substrates. In particular, the argument giving contribution (3) of other grains on the substrate to the depolarization field within each grain is independent of the details of the shape and local environment of the individual grains. Hence, during the initial stage of growth when the coverage is very low, one should find in general for polar materials which grow by island nucleation and coalescence that  $d\omega_z^2/dt = -2d\omega_{x,y}^2/dt$ , where  $t$  is the growth time.

In order to estimate the time dependence of the IR shifts, we make some further simplifications to our model of growth: we assume that the aspect ratio of the grains does not change during the initial growth process, i.e., prior to coalescence of the grains. In this case, the local contributions (1) and (2) to the depolarization field within each grain discussed above will be constant. Only contribution (3) above, i.e., due to the dipole fields of the other grains, will change with time. At very low cubic BN coverage, i.e., when the cubic BN initially nucleates, the dipole fields of the other grains will be negligible. Assuming that the grains are approximately spherical, and that contribution (2) of the inter-

face charges is small, then the local contributions to the depolarization field will be  $\varepsilon_{x,y,z} = -4\pi P_{x,y,z}/3$ , and the frequency of all modes for very low cubic BN coverage will be approximately equal to the Fröhlich frequency,<sup>13</sup>  $\omega_F = \sqrt{2\omega_T^2/3 + \omega_L^2/3}$ .

For a constant rate of cubic BN growth, the radius  $a$  of the grains will be proportional to  $t^{1/3}$ , where  $t$  is the time since initial nucleation of the cubic BN grains, and the average dipole strength per unit area of the substrate is proportional to  $t$ . We then integrate Eq. (3) over radii  $r > 2a$  (i.e., assuming nonoverlapping grains) to obtain a total contribution to the depolarization field from other grains on the substrate which is proportional to  $t^{2/3}$ .

Defining a coalescence time  $t_c$  as the time required for the grains to coalesce into a uniform layer of cubic BN, and noting that  $\omega_{x,y} \rightarrow \omega_T$  and  $\omega_z \rightarrow \omega_L$  as  $t \rightarrow t_c$ , we find that the time dependence of the mode frequency  $\omega_{x,y}$  for polarization parallel to the substrate is given by

$$\omega_{x,y}^2 = \frac{1 - (t/t_c)^{2/3}}{3} \omega_L^2 + \frac{2 + (t/t_c)^{2/3}}{3} \omega_T^2 \quad \text{for } t < t_c, \quad (4a)$$

and the mode frequency  $\omega_z$  for polarization normal to the substrate is given by

$$\omega_z^2 = \frac{1 + 2(t/t_c)^{2/3}}{3} \omega_L^2 + \frac{2 - 2(t/t_c)^{2/3}}{3} \omega_T^2 \quad \text{for } t < t_c. \quad (4b)$$

For  $t > t_c$ ,  $\omega_{x,y} = \omega_T$  and  $\omega_z = \omega_L$ . As we shall see in Sec. V, below, this model agrees well with the observed dependence of the mode shifts during the initial stages of growth. We note that this model does not assume that the grains are uniform in size over the substrate—only that their aspect ratio does not change much after initial nucleation.

#### IV. THEORY OF SHIFTS DUE TO STRAIN

The calculated strain shifts of the TO-phonon frequencies<sup>28,29</sup> and calculated elastic constants<sup>30,31</sup> of bulk cubic BN allow us to estimate the effects of film strain alone on the IR-absorption peaks. For a cubic material, there are three independent elastic coefficients<sup>30,31</sup> and three independent coefficients of the phonon shifts.<sup>28,29</sup> One irreducible component of the strain corresponds to isotropic strain  $\epsilon_{\text{iso}}$  of the crystal, a second to uniaxial, traceless strain  $\epsilon_{[001]}$  ( $E$  is the irreducible representation) along the [001] direction, and a third component to uniaxial, traceless strain  $\epsilon_{[111]}$  ( $T_2$  is the irreducible representation) along the [111] direction. Experimental values<sup>32–35</sup> of the bulk modulus  $B$  of cubic BN are in the range 369–382 GPa. The single-crystal shear elastic constant  $C_{44}$  has a measured value<sup>33</sup> of 480 GPa, and the other independent shear elastic constant  $C_s$  can be obtained from the measured values<sup>35</sup> of the elastic constants  $C_{11} = 820$  GPa and  $C_{12} = 190$  GPa, as  $C_s = (C_{11} - 2C_{12})/2 = 315$  GPa. These coefficients have been calculated using pseudopotential plane-wave, total-energy methods<sup>30</sup> as  $B = 386$  GPa,  $C_s = 326$  GPa, and  $C_{44} = 483$  GPa, and using all-electron, full-potential linear muffin-tin orbital methods<sup>31</sup> as  $B = 400$  GPa,  $C_s = 327$  GPa, and  $C_{44} = 493$  GPa. We calculated these coefficients independently, using linear combina-

tion of Gaussian orbitals total-energy methods, as described in Ref. 28, and found values of  $B=375$  GPa,  $C_s=326$  GPa, and  $C_{44}=486$  GPa, in excellent agreement with experimental measurements and with other calculations.

As discussed in Sec. II, above, SFM images indicate that during the initial growth of the cubic BN, the grains are oriented with their [111] axis normal to the substrate. We may assume that the normal component of the stress at the surface of the film is zero. The strain in the microcrystallites oriented with their [111] axes normal to the substrate with no normal stress on their free surface may be made up of an isotropic strain component of magnitude  $\epsilon_{\text{iso}}$  and a  $T_2$  irreducible, traceless strain component of magnitude  $\epsilon_{[111]}$ . For the stress on the free surface to be zero, the strain components must satisfy  $\epsilon_{\text{iso}}/\epsilon_{[111]} = -3B/(2C_{44}) = -1.153$ .

The strain parallel to the substrate is  $\epsilon_{x,y} = \epsilon_{\text{iso}} - \epsilon_{[111]}/2$ . The TO-phonon shift for modes with polarization parallel to the substrate is given by

$$\Delta\omega_{x,y} = \frac{d\omega}{d\epsilon_{\text{iso}}} \epsilon_{\text{iso}} - \frac{1}{2} \frac{d\omega}{d\epsilon_{[111]}} \epsilon_{[111]},$$

and the TO-phonon shift for modes with polarization normal to the substrate is given by

$$\Delta\omega_z = \frac{d\omega}{d\epsilon_{\text{iso}}} \epsilon_{\text{iso}} + \frac{d\omega}{d\epsilon_{[111]}} \epsilon_{[111]}.$$

Using the irreducible strain shifts,<sup>28,29</sup> we find a shift  $d\omega_{x,y}/d\epsilon_{x,y} = -34 \text{ cm}^{-1}$  per 1% strain parallel to the surface for phonon modes with polarization parallel to the substrate, and a much smaller shift  $d\omega_z/d\epsilon_{x,y} = -4 \text{ cm}^{-1}$  per 1% strain parallel to the surface for phonon modes with polarization normal to the substrate.

For a cubic BN thin film with randomly oriented microcrystallites, it is not possible to calculate the elastic constants and phonon strain shifts exactly, since the stress-strain relations depend on the shapes of grains within the material.<sup>36</sup> However, we can make an estimate of the elastic constants for the randomly oriented material by a spherical average of the irreducible components of the cubic system. This gives an estimate for the shear modulus  $\bar{C}_s = \bar{C}_{44} = (3C_{44} + 2C_s)/5 = 422$  GPa for the randomly oriented material. (This estimate is based on the approximation that the strain is microscopically uniform throughout the material, and the shear modulus so obtained is an upper bound for the actual value of the shear modulus.) A similar isotropic averaging of the phonon shifts for the randomly oriented material gives an average shift of  $-17.6 \text{ cm}^{-1}$  of modes with polarization along the strain for 1% traceless uniaxial strain, and  $+8.8 \text{ cm}^{-1}$  for modes with polarization perpendicular to the strain. Using these estimates for the randomly oriented material, we find that the frequency shift of modes with polarization normal to the film is approximately  $-7 \text{ cm}^{-1}$  for 1% strain parallel to the film surface, whereas the mode with polarization parallel to the film has a frequency shift of  $-29 \text{ cm}^{-1}$  per 1% strain.

The above calculation of the mode frequency shift due to strain for polarization normal to the film assumes that changes in the transverse charge for the zone-center modes and the optical dielectric constant combine to give a bulk LO-TO splitting which is not strain dependent. This has been

shown<sup>23</sup> to be approximately true in bulk cubic BN for isotropic strain, but has not been measured for uniaxial strains.

## V. DISCUSSION AND CONCLUSIONS

From the experimental results and theoretical analyses presented above, the following overall picture of the mode frequency shifts during nucleation and growth of cubic BN emerges. At the initial nucleation stage the long-wavelength infrared radiation polarizes small separated cubic BN crystallites, leading to a long-range depolarization electric field. The effect of this field is seen as a shift in the TO-phonon frequency. As the islands coalesce to form a continuous film, the depolarization field for mode polarization parallel to the substrate surface rapidly vanishes, and the TO mode returns to an equilibrium value. The remaining small shift in the TO mode is a measure of the strain of the cubic BN layer. At the same time, the depolarization field for mode polarization normal to the surface becomes equal to that for a uniform film of cubic BN, and the mode frequency tends to the bulk LO value. We will show that this interpretation is compatible in every detail with measurements of infrared absorbance at off-normal incidence, whereas the expected effects of frequency shifts due to strain alone are not.

The very small ratio  $\Delta\omega_z/\Delta\omega_{x,y} = 0.12-0.24$  calculated (see Sec. IV, above) for the frequency shifts due to strain of modes with polarization normal to and parallel to the substrate is in agreement with our measurements of the peak shifts at off-normal incidence in thicker, more uniform films of cubic BN (see Table I and Fig. 3). For thicker films the peak near the bulk cubic BN TO position shows a small systematic shift to higher frequencies with increasing film thickness, while the mode near the bulk cubic BN LO position (i.e., the mode with polarization normal to the surface) shows no discernable shift. Moreover, when such films are delaminated from their substrate, the TO mode frequency returns to the bulk, unstrained value of  $1065 \text{ cm}^{-1}$ . This leads us to ascribe frequency shifts for thicker films to the effects of strain. The value  $\omega_T = 1077 \text{ cm}^{-1}$ , found in the films immediately after coalescence, would indicate a compressive strain of 0.35–0.4% parallel to the surface, based on the strain coefficients calculated in Sec. IV above. Moreover, we have found<sup>37</sup> that residual film strain decreases dramatically with growth temperature, resulting in a decrease in the cubic TO-phonon shift by  $2 \text{ cm}^{-1}$  per  $100^\circ\text{C}$  increase in growth temperature above  $800^\circ\text{C}$ .

However, during the initial stage of nucleation and growth of cubic BN, when the film consists of separated grains of cubic BN, the model presented in Sec. III leads us to expect large shifts in the frequency of the mode polarized normal to the surface, in contrast to the relatively small shift expected in strained homogeneous films. Considering the complications of the system geometry which occur in the real growth process, the experimental results are in remarkably good agreement with the detailed predictions of this model.

The ratios of the (negative) shift of the  $\omega_L^2$  to the (positive) shift of the  $\omega_T^2$  at the initial stages of growth, as found in the off-normal absorption experiments, are listed in Table I. We assume that the *c*-BN islands have a small intrinsic strain at early nucleation equal to that found immediately

after coalescence (i.e., the TO frequency shift equals the measured TO frequency minus a strained equilibrium frequency of  $\omega_T = 1077 \text{ cm}^{-1}$ ). A ratio  $\Delta(\omega_L^2)/\Delta(\omega_T^2) = 2$  is expected from the islanding effects discussed in Sec. III for samples at the early stages of nucleation, when the cubic BN grains are well separated. This is seen consistently in those samples where the shifts are sufficiently large to be reliably measured within the resolution of the FTIR spectrometer. The dashed line in Fig. 3 is a plot of  $\omega_T = \omega_{x,y}$  in Eq. (4a) versus the growth time of cubic BN, using a coalescence time  $t_c = 110 \text{ min}$ . This coalescence time was determined by subtracting the time at which the growth of cubic BN starts (i.e., when the hexagonal BN layer is  $300 \text{ \AA}$  thick, as indicated by TEM images) from the time at which the film coalesces (i.e., the time after which the frequency shift remains approximately constant). This coalescence time agrees well with the growth and coalescence of grains indicated in SFM images. The time axis in Fig. 3 is measured from the time at which cubic BN growth begins. We note that for very short growth times the absorption peaks are difficult to resolve due to the very low coverage of cubic BN.

In conclusion, we find no evidence in the IR-absorption peak shifts to support the theory that cubic boron nitride nucleates at a time of exceptionally high strain, or that large compressive strain is a driving force for the hexagonal-to-cubic transition. Rather, we find that the very large frequency shifts that occur during early growth indicate the nucleation of small cubic BN grains when the hexagonal BN film is approximately  $300 \text{ \AA}$  thick. Based on the time it takes

to form a continuous cubic layer (110 min after the growth of the amorphous and hexagonal layers), the nucleation sites are separated from each other by  $\approx 500 \text{ \AA}$ , and coalesce to form an approximately uniform layer when the grain size equals the average separation of the nucleation sites. This is consistent with the average grain size we measure from TEM dark-field image analysis and SFM images. While the results suggest that a small amount of compressive strain (0.35–0.4%) is present at initial nucleation, this strain is smaller than that observed in thicker films. Moreover, regardless of the decrease in residual film strain (to values well below that needed for bulk-phase thermodynamic stability of cubic BN) at higher growth temperatures, we continue to see the amorphous-hexagonal-cubic morphology, further indicating that strain has little to do with the formation of cubic BN films. We note that the present results for the shifts of the IR-absorption peaks are compatible with the proposal<sup>5</sup> that energetic ions serve to disrupt the *sp*<sup>2</sup>-bonded hexagonal BN material, creating local *sp*<sup>3</sup> bonding sites for the nucleation of the metastable cubic BN.

#### ACKNOWLEDGMENTS

We gratefully acknowledge helpful discussions with R. Merlin and S. A. Solin. The authors also thank S. Kidner for performing the electron microscopy. C.T. and R.C. were supported by the Office of Naval Research through Grant No. N00014-94-J-0763.

\*Electronic address: stephen\_fahy@bureau.ucc.ie

<sup>1</sup>R. H. Wentorf, *J. Chem. Phys.* **26**, 956 (1957).

<sup>2</sup>M. Mieno and T. Yoshida, *Surf. Coat. Technol.* **52**, 87 (1992).

<sup>3</sup>A. K. Ballal, L. Salamanca-Riba, G. L. Doll, C. A. Taylor, and R. Clarke, *J. Mater. Res.* **7**, 1618 (1992).

<sup>4</sup>D. J. Kester and R. Messier, *J. Appl. Phys.* **72**, 504 (1992).

<sup>5</sup>S. Kidner, C. A. Taylor II, and R. Clarke, *Appl. Phys. Lett.* **64**, 1859 (1994).

<sup>6</sup>D. L. Medlin, T. A. Friedmann, P. B. Mirkarimi, P. Rez, M. J. Mills, and K. F. McCarty, *J. Appl. Phys.* **76**, 295 (1994).

<sup>7</sup>M. Kuhr, S. Reinke, and W. Kulisch, *Diam. Relat. Mater.* **4**, 375 (1995).

<sup>8</sup>D. J. Kester, K. S. Ailey, R. F. Davis, and K. L. More, *J. Mater. Res.* **8**, 1213 (1993).

<sup>9</sup>D. R. McKenzie, *J. Vac. Sci. Technol. B* **11**, 1928 (1993).

<sup>10</sup>P. B. Mirkarimi, K. F. McCarty, D. L. Medlin, W. G. Wolfer, T. A. Friedmann, E. J. Klaus, G. F. Cardinale, and D. G. Howitt, *J. Mater. Res.* **9**, 2929 (1994).

<sup>11</sup>D. L. Medlin, T. A. Friedmann, P. B. Mirkarimi, M. J. Mills, and K. F. McCarty, *Phys. Rev. B* **50**, 7884 (1994).

<sup>12</sup>T. A. Friedmann, P. B. Mirkarimi, D. L. Medlin, K. F. McCarty, E. J. Klaus, D. R. Boehme, H. A. Johnson, M. J. Mills, D. K. Ottesen, and J. C. Barbour, *J. Appl. Phys.* **76**, 3088 (1994).

<sup>13</sup>H. Fröhlich, *Theory of Dielectrics* (Clarendon, Oxford, 1949).

<sup>14</sup>R. Ruppini and R. Englman, *Rep. Prog. Phys.* **33**, 149 (1970).

<sup>15</sup>M. P. Chamberlain, C. Trallero-Giner, and M. Cardona, *Phys. Rev. B* **51**, 1680 (1995).

<sup>16</sup>E. Roca, C. Trallero-Giner, and M. Cardona, *Phys. Rev. B* **49**, 13 704 (1994).

<sup>17</sup>C. Trallero-Giner, F. Comas, and F. Garcia-Moliner, *Phys. Rev. B* **50**, 1755 (1994).

<sup>18</sup>D. W. Berreman, *Phys. Rev.* **130**, 2193 (1963).

<sup>19</sup>P. J. Gielisse, S. S. Mitra, J. N. Plendl, R. D. Griffis, L. C. Mansur, R. Marshall, and E. A. Pascoe, *Phys. Rev.* **155**, 1039 (1967).

<sup>20</sup>D. M. Hoffman, G. L. Doll, and P. C. Eklund, *Phys. Rev. B* **30**, 6051 (1984).

<sup>21</sup>R. Geick, C. H. Perry, and G. Rupprecht, *Phys. Rev.* **146**, 543 (1966).

<sup>22</sup>O. Brafman, G. Lengyel, S. S. Mitra, P. J. Gielisse, J. N. Plendl, and L. C. Mansur, *Solid State Commun.* **6**, 523 (1968).

<sup>23</sup>J. A. Sanjurjo, E. Lopez-Cruz, P. Vogl, and M. Cardona, *Phys. Rev. B* **28**, 4579 (1983).

<sup>24</sup>J. S. Blakemore, *Solid State Physics*, 2nd ed. (Cambridge University Press, Cambridge, 1985), p. 420.

<sup>25</sup>C. Kittel, *Introduction to Solid State Physics*, 7th ed. (Wiley, New York, 1996), p. 384.

<sup>26</sup>J. D. Jackson, *Classical Electrodynamics*, 2nd ed. (Wiley, New York, 1975), pp. 147–9.

<sup>27</sup>E. M. Purcell, *Electricity and Magnetism*, 2nd ed. (McGraw-Hill, New York, 1985), p. 356.

<sup>28</sup>S. Fahy, *Phys. Rev. B* **51**, 12873 (1995); **53**, 11 884(E) (1996).

<sup>29</sup>M. Cardona and E. Anastassakis, *Phys. Rev. B* **54**, 14 888 (1996).

<sup>30</sup>P. Rodriguez-Hernandez, M. Gonzalez-Diaz, and A. Munoz, *Phys. Rev. B* **51**, 14 705 (1995).

<sup>31</sup>K. Kim, W. R. L. Lambrecht, and B. Segall, *Phys. Rev. B* **53**, 16 310 (1996).

<sup>32</sup>E. Knittle, R. M. Wentzcovitch, R. Jeanloz, and M. L. Cohen, *Nature (London)* **337**, 349 (1989).

<sup>33</sup>I. V. Aleksandrov, A. F. Goncharov, S. M. Stishov, and E. V.

- Yakovenko, Pis'ma Zh. Eksp. Teor. Fiz. **50**, 116 (1989) [JETP Lett. **50**, 127 (1989)].
- <sup>34</sup>A. D. Alvarenga, M. Grimsditch, and A. Polian, J. Appl. Phys. **72**, 1955 (1992).
- <sup>35</sup>M. Grimsditch, E. S. Zouboulis, and A. Polian, J. Appl. Phys. **76**, 832 (1994).
- <sup>36</sup>See, for example, A. E. Green and W. Zerna, *Theoretical Elasticity* (Clarendon, Oxford, 1954).
- <sup>37</sup>C. A. Taylor II and R. Clarke, in *III-Nitride, SiC and Diamond Materials for Electronic Devices*, edited by D. K. Gaskill, C. D. Brandt, and R. J. Nemanich, MRS Symposia Proceedings No. 423 (Materials Research Society, Pittsburgh, 1996).